JOURNAL OF AEROSPACE COMPUTING, INFORMATION, AND COMMUNICATION
Vol. 3, April 2006

Implementation of Template-Based Image Registration for Aerodynamic Testing

Wim Ruyten*
Euclidean Optics Inc., Tullahoma, Tennessee 37388-6471

A mathematical model is described that underlies image registration of digital images of test articles in aerodynamic testing, in which registration targets are used to establish the relationship between 2D image coordinates and 3D model coordinates. Specifically, it is shown how search templates can be computed for individual targets, and how these templates can be used to perform subpixel localization of the desired image features through correlation matching.

I. Introduction

MANY optical techniques are currently of interest for application in aerodynamic testing. For example, in Ref. 1 it was shown how, at the Arnold Engineering Development Center (AEDC), on-line processing of pressure-sensitive paint (PSP) images has been accomplished through developments in software, hardware, and data reduction strategies. It is the purpose of the present paper to document an essential element of such automated processing, namely the use of search templates for finding registration targets in the hundreds or thousands of images that are acquired during a typical test. A detailed theoretical treatment of the use of such templates has been presented previously,[2,3] and it has been demonstrated experimentally that a registration uncertainty better than 0.1 image pixels can be achieved with typical research equipment.[3] What has not been published so far is the algorithm for calculation of the search templates, except in the sense that a former (more elaborate) version of this work was presented previously as a conference paper.[4] For a broader introduction to the challenge of processing PSP images, the reader is referred elsewhere.[1,5–7] This paper addresses specifically the calculation of search templates for correlation matching, a scheme that is also applicable to many other optical techniques that are currently of interest for wind-tunnel testing.[8–10]

II. The Image Registration Challenge

Figure 1 shows an image of a painted F-16 fighter jet model, acquired during a PSP test. Visible in the image are circular registration targets that serve to establish the relationship between 2D image coordinates and 3D model coordinates. Figure 2 shows a schematic of the registration algorithm that is described in Ref. 1: A set of tunnel parameters, including model attitude angles, is used to estimate the position and orientation of the sting-mounted test article with respect to the test facility (block 1 in Fig. 2). When combined with a set of calibration parameters for each camera, this allows a set of mapping coefficients to be calculated (block 2 in Fig. 2) that describe, for any registration target i, the relationship between its 3D model coordinates, $\mathbf{x}_i$, and the resulting image coordinates, (u_i, v_i), expressed in

Received 27 July 2005; revision received 17 January 2006; accepted for publication 18 January 2006.

* Director of Research; Associate Fellow, AIAA; this work was performed while the author was employed as an Engineer Specialist with Aerospace Testing Alliance, the operations, maintenance, information measurement, and support contractor for Arnold Engineering Development Center, Air Force Materiel Command, Arnold Air Force Base, Tullahoma, Tennessee.

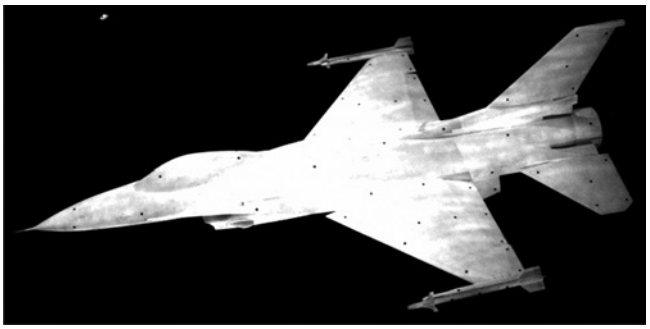

Fig. 1 Image of F-16 test article with registration targets.

image pixels. This relationship may be written symbolically as[1]

$$(u_i, v_i) = \tilde{F}(\mathbf{x}_i) \tag{1}$$

The model coordinates $\mathbf{x}_i$ of the registration targets are typically obtained prior to the test, for example, using a coordinate measuring machine. It is then possible to calculate a search template for each target (block 3 in Fig. 2), allowing each target to be located in the image (block 6 in Fig. 2). Optionally, if a 3D grid of the test article is available (this is typical in PSP measurements), a visibility check can be performed to prevent the algorithm from searching for targets that are occluded (blocks 4 and 5 in Fig. 2). Even so, it is possible that some targets are not found. This is generally not a problem. Once the search for all targets has been completed, a least squares fit is performed that involves the image coordinates of all of the registration targets that were found, to arrive at an updated mapping function F (block 7 in Fig. 2).[7,11]

In the following, it is assumed that a reasonable estimate of the mapping function F [denoted with a tilde in Eq. (1)] is available to serve as a starting point for the image registration task.[4] The challenge of finding a particular target, i, in an image may then be illustrated by Fig. 3, which shows a detail view of a black, round, registration target, which is rendered as a group of darkened image pixels against a light background, with an actual center at point A, an initial position estimate at point B, and a non-digitized elliptical outline that would, in order to be fully resolved (which it never is), require a spatial resolution far greater than the actual resolution in the digital image.

Given the search template, the task of finding the actual location of the registration target in the image involves stepping the search template across the image in the vicinity of the predicted location, finding a point of maximum correlation, and subpixel refinement involving two derivate templates. This is explained in detail in Refs. 2 and 3 and reviewed briefly in Section IV. What is not covered in Refs. 2 and 3 is the actual computation of the search templates. This is the subject of Section III.

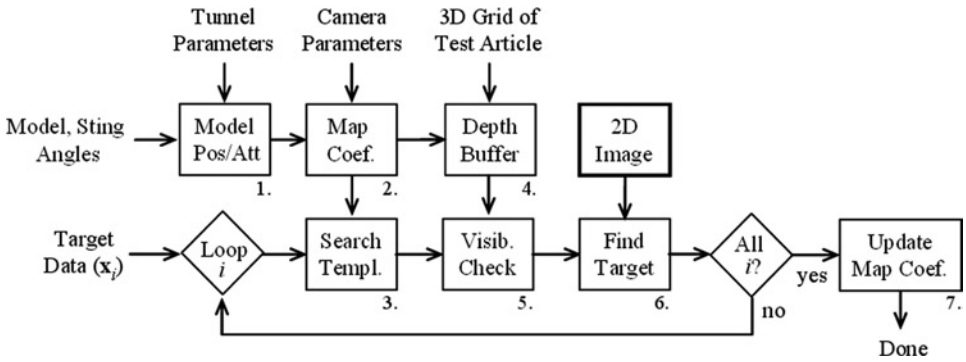

Fig. 2 Image registration flow diagram.

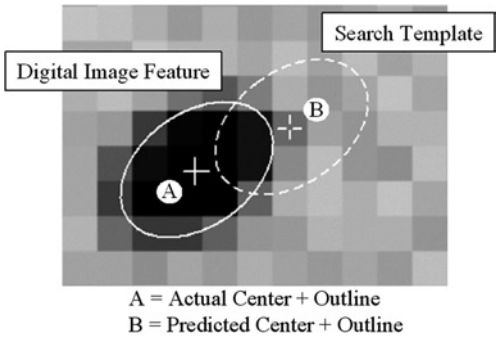

Fig. 3 Illustration of use of search template.

III. Calculation of Search Templates

Figure 4 shows a possible search template for the image feature from Fig. 3. The template consists of an array of occupied pixel fractions, given a pre-selected subpixel placement of the target center. This template is stepped across the image in one pixel increments, in the vicinity of the predicted target location, to find a point of maximum correlation. In this way, the actual location of the target in the image is established to a resolution of one image pixel. This technique is well established in the field of image processing.[12,13] As is shown in Refs. 2 and 3, refinement of this centering scheme to subpixel uncertainty is possible by augmentation of the conventional search template with two derivative templates. These are shown in Fig. 5, for the case of the template from Fig. 4. Essentially, the derivative templates give the change in occupied pixel fractions from Fig. 4 for an infinitesimal (i.e., subpixel) shift of the template, as explained below.

Let us now turn to the calculation of the templates. For some target i, let $\{\mathbf{x}_{ij}\}$ denote a set of n points on the perimeter of the target, with $j = 1, \ldots, n$. Typical values of n are 45 or 90. For a circular target with radius r_i and position $\mathbf{x}_i$ in model space, the target may be approximated as an n-sided regular polygon with perimeter points $\{\mathbf{x}_{ij}\}$

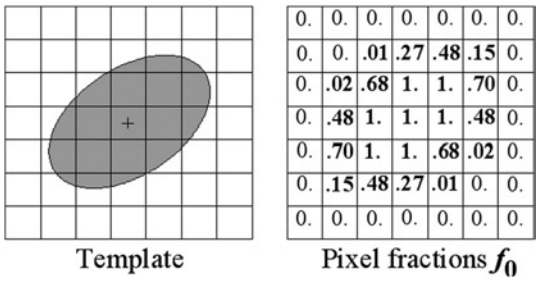

Template

0.	0.	0.	0.	0.	0.	0.
0.	0.	.01	.27	.48	.15	0.
0.	.02	.68	1.	1.	.70	0.
0.	.48	1.	1.	1.	.48	0.
0.	.70	1.	1.	.68	.02	0.
0.	.15	.48	.27	.01	0.	0.
0.	0.	0.	0.	0.	0.	0.

Pixel fractions f_0

Fig. 4 Example of conventional search template.

0.	0.	0.	0.	0.	0.	0.
0.	0.	-.05	-.40	.02	.43	0.
0.	-.23	-.77	0.	0.	1.	0.
0.	-1.	0.	0.	0.	1.	0.
0.	-1.	0.	0.	.77	.23	0.
0.	-.43	-.02	.40	.05	0.	0.
0.	0.	0.	0.	0.	0.	0.

Derivatives f_u

0.	0.	0.	0.	0.	0.	0.
0.	0.	.07	1.	1.	.55	0.
0.	.17	.93	0.	0.	.13	0.
0.	.51	0.	0.	0.	-.51	0.
0.	-.13	0.	0.	-.93	-.17	0.
0.	-.55	-1.	-1.	-.07	0.	0.
0.	0.	0.	0.	0.	0.	0.

Derivatives f_v

Fig. 5 Augmented templates corresponding to Fig. 4.

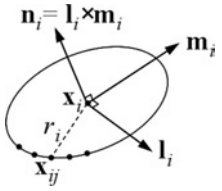

Fig. 6 Geometry for calculating perimeter points of circular template.

given by:

$$\mathbf{x}_{ij} = \mathbf{x}_i + r_i' \left[\mathbf{l}_i \cos\left(\frac{2\pi j}{n}\right) + \mathbf{m}_i \sin\left(\frac{2\pi j}{n}\right) \right] \tag{2}$$

where $\mathbf{l}_i$ and $\mathbf{m}_i$ are unit tangent vectors at the surface of the target at point $\mathbf{x}_i$ (see Fig. 6) and r_i' is the radius of the target, with a correction factor applied to render the surface area of the n-sided regular polygon equal to that of the actual target. That is

$$r_i' = r_i \left[\frac{2\pi/n}{\sin(2\pi/n)} \right]^{1/2} \tag{3}$$

For $n = 45$ or $n = 90$, the correction factor from Eq. (3) is practically negligible, but in calculations in which speed is of the essence, it can be imagined that a much smaller value of n would be used, while sacrificing centering uncertainty. The specific choice of tangent vectors $\mathbf{l}_i$ and $\mathbf{m}_i$ in Eq. (2) and Fig. 6 is not important, so long as the two are orthogonal, that is, $(\mathbf{l}_i \bullet \mathbf{m}_i) = 0$, and their vector product is equal to the surface normal, $\mathbf{n}_i$, of the target, that is, $\mathbf{n}_i = \mathbf{l}_i \times \mathbf{m}_i$. Implicit in Eq. (2) is the assumption that the surface is flat on the scale of the target.

Using Eq. (1), a corresponding set of n image coordinates (u_{ij}, v_{ij}) may be calculated for the n spatial coordinates $\mathbf{x}_{ij}$. By interpolation, this set of projected perimeter points can be expanded into a K-sided polygon (with $K > n$), such that each line segment is contained inside a single image pixel (see Fig. 7). Let (u_{k-1}, v_{k-1}) and (u_k, v_k) be the end points of the k-th line segment, with $(u_0, v_0) = (u_K, v_K)$, and let (p_k, q_k) denote the coordinate indices of the pixel in which the k-th line segment is contained. The partial contribution of line segment k to the occupied pixel fraction $f_0(p_k, q_k)$ is then given by the trapezoidal area

$$\Delta f_{0k}(p_k, q_k) = (u_{k-1} - u_k) \left(\frac{v_k + v_{k-1}}{2} - q_k \right) \tag{4}$$

This is not the only contribution to the template for this line segment. Rather, imagine that the k-th line segment contributes area fractions to the entire column of pixels shaded in Fig. 7. For pixels with vertical index $q < q_k$, these

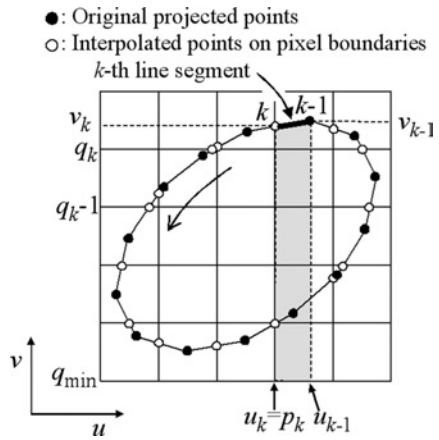

Fig. 7 Calculation of template from polygonal curve.

area fractions are given by

$$\Delta f_{0k}(p_k, q) = u_{k-1} - u_k, \quad q < q_k \tag{5}$$

The fractional contributions from Eqs. (4) and (5) can be either positive (at the top of the loop in Fig. 7) or negative (at the bottom of the loop). However, when contributions are summed for all line segments k, the resulting occupied pixel fractions for all pixels (p, q) will be nonnegative, provided the projected outline of the target is traversed in counter-clockwise direction. Specifically, the resulting occupied pixel fraction for a pixel (p, q) may be calculated as the sum

$$f_0(p, q) = \sum_{k \in (p,q)} \sum_{q'=q_{\min}}^{q_k} \Delta f_{0k}(p_k, q') \tag{6}$$

where $q_{\min}$ represents the lowest value of q that is of interest in the calculation of the template.

To calculate the derivative templates from Fig. 5, observe that, in Fig. 4, the change in the fractional contribution Δf_{0k} for pixel (p_k, q_k) due to an infinitesimal shift δu of the template along the u-axis is given by $(v_k - q_k)\delta u$ as is illustrated by the shaded area in Fig. 8a. If, instead of the left side of the trapezoidal area element being aligned with a pixel edge, the right side were aligned with an edge (see Fig. 8b), the change in area would be $-(v_{k-1} - q_k)\delta u$. For a general element k, the fractional change in the occupied pixel fraction Δf_{0k} due to a shift of the template along the horizontal image axis thus gives rise to the following fractional contribution to the derivative template f_u

$$\Delta f_{uk}(p_k, q_k) = \theta_k(v_k - q_k) - \theta_{k-1}(v_{k-1} - q_k) \tag{7}$$

Here the values of the factors θ are either 1 or 0, depending on whether the corresponding values of u_k and u_{k-1} are or are not aligned with a pixel edge, respectively. Likewise in Fig. 7, a displacement of the template by an infinitesimal shift δv in the vertical direction (see Fig. 8c) would change the area fraction of the trapezoidal element Δf_{0k} by an amount $(u_{k-1} - u_k)\delta v$. The partial contribution of line segment k to the derivative template f_v can thus be calculated as

$$\Delta f_{vk}(p_k, q_k) = u_{k-1} - u_k \tag{8}$$

The resulting augmented template values f_u and f_v are found by summing the fractional contributions of all line elements, giving

$$f_\lambda(p, q) = \sum_{k \in (p,q)} \Delta f_{\lambda k}(p_k, q_k), \quad \lambda = u, v \tag{9}$$

These values are in the range -1 to $+1$ for each pixel (see Fig. 5). The reader may confirm that the same set of template values f_u is obtained if, in Eq. (7), the factors θ (and hence the factors q_k) are omitted, yielding the simplified expression

$$\Delta f'_{uk}(p_k, q_k) = v_k - v_{k-1} \tag{10}$$

The reason that Eq. (10) sums to the same result in Eq. (9) is that, to the extent that Eq. (10) is no longer strictly the rate of change of the occupied pixel fraction Δf_{0k} for a horizontal shift of the template, the "error" in this fractional shift is canceled out by an equal and opposite error for one or more other elements k that are located inside the same pixel (p_k, q_k).

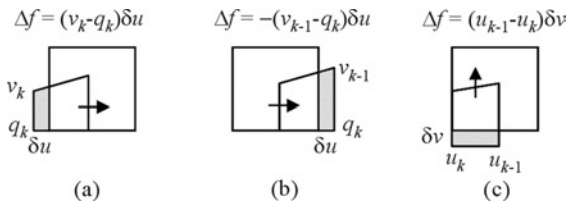

Fig. 8 Calculation of augmented terms from infinitesimal shifts of template.

Another "proof" for the correctness of Eq. (10) is to observe that, instead of column summing in Eq. (6) and Fig. 7, row-summing might be used, which would interchange the roles of the horizontal and vertical indices. By this symmetry argument, the partial contributions in Eqs. (8) and (10) must, indeed, be expressable in equivalent fashion.

The algorithm for the calculation of the search templates can now be summarized as follows: (1) Calculate the projected target perimeter points from Eqs. (1)–(3) and interpolate the connecting line segments on pixel boundaries; (2) Select a rectangular area of pixels that encloses this projection; (3) Initialize the three templates (f_0, f_u, and f_v) to zero; (4) Add, for each perimeter segment k, the following contributions to the templates: (4a) the fraction Δf_{0k} from Eq. (5) for pixel (p_k, q_k); (4b) the fractions Δf_{0k} from Eq. (6) for pixels (p_k, q) with $q < q_k$; (4c) the fractions $\Delta f'_{uk}$ from Eq. (9) for pixel (p_k, q_k); and (4d) the fractions Δf_{vk} from Eq. (8) for pixel (p_k, q_k). Note the remarkable efficiency of this algorithm, in that only a single multiplication [from Eq. (4)] is required for each line segment.

As a final comment on the calculation of the search templates: In principle (as suggested by a reviewer), the occupied pixel fractions might be calculated analytically. This is possible (though cumbersome) for the special case in which a target is viewed exactly normally, and the projected target is rendered as a circle. However, in general, the projected target will be rendered as a tilted ellipse, which requires the use of special functions (so-called elliptical integrals). These are much more difficult to implement than the polygonal scheme described here and would be slower during actual computation.

IV. Use of the Search Templates

In a sense, Section III concludes the presentation of previously unpublished results on the implementation of augmented template matching. However, the main results from Refs. 2 and 3 are summarized below, so as to illustrate how the templates from Section III are used in practice. First, observe (see Fig. 9) that there are ten possible cross-correlation sums between the three members of the augmented template (the sets of numbers f_0, f_u, and f_v from Figs. 4 and 5) and the image feature from Fig. 3 (the "scene"), which is denoted here by the matrix of pixel values g. Each of the ten sums from Fig. 9 is calculated according to the formula

$$S_{AB} \equiv \sum_{p,q} [A(p,q) - \langle A \rangle] [B(p,q) - \langle B \rangle] \tag{11}$$

where both A and B can represent either f_0, f_u, f_v, or g and where the angle brackets denote average values across the template. (In Fig. 9 and below, subscripts f, u, and v on S denote the template terms f_0, f_u, and f_v respectively.)

In conventional template matching, only three of the ten correlation sums from Fig. 9 are used (those from the lower part of Fig. 9). In this conventional scheme, the template is stepped across the scene in increments of one pixel in both directions until a point of maximum normalized correlation is found. This normalized correlation is defined as

$$J_{fg}(\Delta p, \Delta q) \equiv \frac{S_{fg}^2}{S_{ff} S_{gg}} \quad (\text{with } 0 \le J_{fg} \le 1). \tag{12}$$

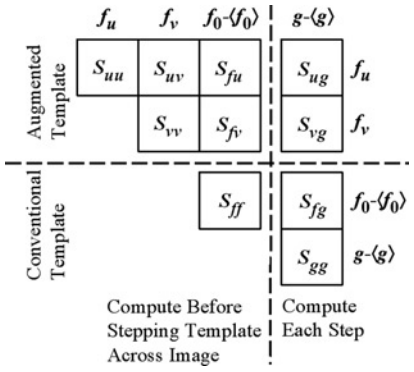

Fig. 9 Correlation sums arising in conventional and augmented template searches.

Here Δp and Δq denote the integer-pixel shifts between the initial position of the template and the trial positions for which the normalized correlation from Eq. (12) is evaluated. Perfect correlation (with $J_{fg} = 1$) cannot normally be obtained in this manner, even in the absence of noise, because the required shift of the template would require noninteger values of Δp and Δq. This is where the augmented template technique comes in. Once a point of maximum correlation is found for some set of integer shifts Δp and Δq, a subpixel centering refinement can be calculated from the augmented template terms by solution of the linear system

$$\begin{pmatrix} S_{uu} & S_{uv} \\ S_{uv} & S_{vv} \end{pmatrix} \begin{pmatrix} \Delta u \\ \Delta v \end{pmatrix} = \frac{S_{ff}}{S_{fg}} \begin{pmatrix} S_{ug} \\ S_{vg} \end{pmatrix} - \begin{pmatrix} S_{fu} \\ S_{fv} \end{pmatrix} \tag{13}$$

This yields the required subpixel centering refinement $(\Delta u, \Delta v)$, which, when combined with the previously established integer shifts Δp and Δq, yields a more accurate determination of the center of the registration target in the image. A further refinement may be obtained by recalculating the search template at the newly found position, and solving Eq. (13) anew. For further details on the derivation of these results, as well as the theoretical and experimental study of the uncertainty of the resulting registration scheme, the reader is referred to Refs. 2 and 3.

V. Conclusion

The image registration algorithm that is shown schematically in Fig. 2 has been used extensively as the enabling step for automatic processing of thousands of PSP images from AEDC's 16-ft Transonic Wind Tunnel.[1] Detailed performance results of the template-based search algorithms are documented in Ref. 3. Use of the augmented template technique typically results in 99% or more of visible registration targets being found correctly, with a root-mean-square uncertainty on the order of 0.05–0.10 image pixels.[3] Both the success rate and the centering uncertainty of the template-based scheme are a notable improvement over an earlier scheme that relied on blob finding and centroiding.[14] In particular, the difficulty of identifying, for each target individually, appropriate threshold levels (to distinguish the target from the surrounding background) is avoided altogether in the template-based scheme. Moreover, the template-based scheme is very unlikely to lock onto spurious image features in the vicinity of the sought-after target. Lastly, the performance of the template-based scheme is not particularly dependent on the size of the registration targets, so long as they are rendered with reasonable contrast in the image at a diameter of two or more image pixels. This allows relatively small registration targets to be used (a diameter of a few image pixels is adequate) in those applications in which the goal of the measurement is to map the surface of the test article as completely as possible, as is the case in PSP testing.

Acknowledgments

The author would like to acknowledge discussions with William Lawrence, Marvin Sellers and Daryl Sinclair, as well as the inputs from the anonymous referees. This work was supported in part by funding from the Test and Evaluation Program of the Air Force Office of Scientific Research, managed by Drs. Neal Glassman and John Schmisseur.

References

[1]Ruyten, W., and Sellers, M., "On-Line Processing of Pressure-Sensitive Paint Images," *Journal of Aerospace Computing, Information, and Communication*, Vol. 1, September 2004, pp. 372–382.

[2]Ruyten, W., "Subpixel Localization of Synthetic References in Digital Images by Use of an Augmented Template," *Optical Engineering*, Vol. 41, No. 3, 2002, pp. 601–607.

[3]Ruyten, W., "Extension of Subpixel Augmented Template Matching to Imperfectly Rendered Binary Targets," *Optical Engineering*, Vol. 43, No. 3, March 2004, pp. 639–647.

[4]Ruyten, W., "Automatic Image Registration for Optical Techniques in Aerodynamic Test Facilities," AIAA Paper 2004-2400, June 2004.

[5]Bell, J. H., Schairer, E. T., Hand, L. A., and Mehta, R. D., "Surface Pressure Measurements Using Luminescent Coatings," *Annual Review of Fluid Mechanics*, Vol. 33, 2001, pp. 155–206.

[6]Bell, J. H., and McLachlan, B. G., "Image Registration for Pressure-Sensitive Paint Applications," *Experiments in Fluids*, Vol. 22, No. 1, 1996, pp. 78–86.

[7]Liu, T., Cattafesta, L. N., III, Radeztsky, R. H., and Burner, A. W., "Photogrammetry Applied to Wind Tunnel Testing," *AIAA Journal*, Vol. 38, No. 6, 2000, pp. 964–971.

[8]ICIASF 2003 Record, *20th International Congress on Instrumentation in Aerospace Simulation Facilities*, Göttingen, Germany, August 25–29, 2003.

[9]Schairer, E. T., and Hand, L. A., "Measurements of Unsteady Aeroelastic Model Deformation by Stereo Photogrammetry," *Journal of Aircraft*, Vol. 36, No. 6, 1999, pp. 1033–1040.

[10]Ruyten, W., "Model Attitude Determination in a Wind Tunnel with a Luminescent Paint Data System," *AIAA Journal*, Vol. 38, No. 9, 2000, pp. 1692–1697.

[11]Ruyten, W., "More Photogrammetry for Wind-Tunnel Testing," *AIAA Journal*, Vol. 40, No. 7, 2002, pp. 1277–1283.

[12]Foley, J. D., and Van Dam, A., *Fundamentals of Interactive Computer Graphics*, Addison-Wesley, Reading, MA, 1982, pp. 560–561.

[13]Fernàndez, X., and Amat, J., "Detection of small-size synthetic references in scenes acquired with a pixilated device," *Optical Engineering*, Vol. 36, No. 11, 1997, pp. 3073–3080.

[14]Morgan, J. S., Slater, D. C., Timothy, J. G., and Jenkins, E. B., "Centroid position measurements and subpixel sensitivity variations with the MAMA detector," *Applied Optics*, Vol. 28, No. 6, 1989, pp. 1178–1192.